Performance characteristics of low-dissipative generalized Carnot cycles with external leakage losses*

Huang Chuan-Kun(黄传昆)[a], Guo Jun-Cheng(郭君诚)[b]†, and Chen Jin-Can(陈金灿)[a]‡

[a] *Department of Physics, Xiamen University, Xiamen* 361005, *China*
[b] *College of Physics and Information Engineering, Fuzhou University, Fuzhou* 350002, *China*

(Received 21 May 2015; revised manuscript received 18 July 2015; published online 10 October 2015)

Under the assumption of low-dissipation, a unified model of generalized Carnot cycles with external leakage losses is established. Analytical expressions for the power output and efficiency are derived. The general performance characteristics between the power output and the efficiency are revealed. The maximum power output and efficiency are calculated. The lower and upper bounds of the efficiency at the maximum power output are determined. The results obtained here are universal and can be directly used to reveal the performance characteristics of different Carnot cycles, such as Carnot heat engines, Carnot-like heat engines, flux flow engines, gravitational engines, chemical engines, two-level quantum engines, etc.

Keywords: generalized Carnot cycle, low-dissipation, unified model, performance characteristic

PACS: 05.70.Ln, 05.20.–y **DOI:** 10.1088/1674-1056/24/11/110506

1. Introduction

Thermodynamic cycles are of great importance not only in theory but also in practice.[1–8] The Carnot heat engine is one of the most important models in thermodynamics.[9,10] Generalized Carnot cycles have been widely used in the various fields in physics.[11–13] Investigations on the maximum power output of Carnot heat engines and other Carnot cycles and the efficiency at the maximum power output have attracted a great deal of attention during the last few decades and is a hot research topic.[14–17] Recently, Esposito *et al*. established a new cycle model of Carnot heat engines on the basis of the weak dissipation assumption.[16] They proved that the efficiency of low-dissipative Carnot heat engines at the maximum power output is located between $\eta_{\rm C}/2$ and $\eta_{\rm C}/(2-\eta_{\rm C})$, while the Curzon–Ahlborn efficiency[18] $\eta_{\rm CA}=1-\sqrt{1-\eta_{\rm C}}$ can be derived under the so-called symmetric dissipation, where $\eta_{\rm C}$ is the Carnot efficiency. On the basis of Ref. [16], low-dissipation assumption has been successfully used in the models of other thermodynamic cycles such as Carnot refrigerators,[19,20] Carnot chemical engines,[21] two-level quantum Carnot cycles,[22] etc. Many significant results have been obtained from the various low-dissipative cycle models, but the common characteristics of these cycles have been rarely revealed. On the other hand, the external leakage losses of thermodynamic cycles are one of the main sources of irreversible losses,[23–25] but these losses have not been included in the existing low-dissipative cycle models. Thus, it is of great significance to establish a unified model of low-dissipative generalized Carnot cycles with external leakage losses and reveal the general performance characteristics of these cycles.

The rest of the present paper is organized as follows. In Section 2, generalized Carnot cycles are briefly introduced and some examples are given. In Section 3, the model of low-dissipative generalized Carnot cycles with external leakage losses is proposed and the expressions of the power output and the efficiency are derived. In Section 4, the optimal relations between the power output and the efficiency are obtained. In Section 5, the maximum power outputs of cycles operated under different conditions are calculated and the bounds of the efficiency at the power output are determined. In Section 6, the performance characteristics related to the maximum efficiency are also discussed. In Section 7, the performance characteristics of the low-dissipative Carnot heat engine with heat leakage losses are directly obtained from the universal results. Finally, some important conclusions are drawn in Section 8.

2. Generalized Carnot cycles

As is well known, heat engines operated in different temperature fields are able to produce useful work and thermodynamic cycles operated in other potential fields such as the chemical potential field, pressure field, gravitational field, quantum field, etc. are also able to obtain useful work. When thermodynamic cycles are operated in a potential field only including two reservoirs, which may be described by two parameters $X_{\rm H}$ and $X_{\rm C}$ ($X_{\rm H}>X_{\rm C}$), they are usually referred to as generalized Carnot cycles as shown in Fig. 1. Such cycles include four processes, where two processes exchange energy with

*Project supported by the Young Scientists Fund of the National Natural Science Foundation of China (Grant No. 11405032).
†Corresponding author. E-mail: junchengguo@qq.com
‡Corresponding author. E-mail: jcchen@xmu.edu.cn
© 2015 Chinese Physical Society and IOP Publishing Ltd

two reservoirs and the other two processes do not exchange energy with two reservoirs, and can be taken as the models of some heat engines,[13–18,26–28] flux flow engines,[29–31] gravitational engines, chemical engines,[32–35] two-level quantum engines,[36–41] etc. For example, for a Carnot heat engine, $X_{\rm H}$ and $X_{\rm C}$ correspond to the temperatures $T_{\rm H}$ and $T_{\rm C}$ of high- and low-temperature heat reservoirs; for non-Carnot heat engines,[26–28] which include the Otto cycle,[42,43] Brayton cycle,[44–46] Diesel cycle,[47,48] and Atkinson cycle,[49,50] $X_{\rm H}$ and $X_{\rm C}$ correspond to the highest temperature $T_{\rm H}$ and lowest temperature $T_{\rm C}$ of the working substance; for Carnot-like engines such as a gravitational engine, which may be regarded as an abstract model of hydropower stations or tidal power plants, $X_{\rm H}$ and $X_{\rm C}$ correspond to the height $H_{\rm H}$ and $H_{\rm C}$ of high- and low-gravitational potential energy reservoirs. For different types of engines, the parameters corresponding to $X_{\rm H}$ and $X_{\rm C}$ are listed in Table 1, where $\eta_{\rm r,g}$ is the reversible efficiency of generalized Carnot cycles. Some signs in Table 1 are explained as follows. The $F(S_1,S_2)$ is the total entropy change varying with the spin angular momenta $S_i=\langle\hat{S}_z\rangle\,(i=1,2)$,[51–53] $C_{\rm H}$ and $C_{\rm C}$ are the heat capacities of the working substance during two heat exchange processes of non-Carnot heat engines,[26,27,41] T_j $(j=1,2)$ are the initial temperatures of the working substance in two heat exchange processes, and "+" and "−" in signs "±" correspond to the cases of $j=1$ and 2, respectively. The reversible efficiencies $\eta_{\rm r,g}$ of such heat engines and the efficiencies $\eta_{\rm r,m}$ at the maximum work output[41] are listed in Table 2, where $\tau=T_{\rm C}/T_{\rm H}$, $\nu=C_{\rm P}/C_{\rm V}$, and $f=1/(1+\nu)$. The $p_{\rm H}=|a_1|^2$ and $p_{\rm C}=|b_1|^2$ are the probabilities of two different superposed states in the eigenstate $|\phi_1(L)\rangle$, and $\sigma=[i_2^q-(i_2^q-i_1^q)\,|b_1|^2]/[i_2^q-(i_2^q-i_1^q)\,|a_1|^2]$, where i_n $(n=1,2)$ is the quantum number of the system, δ, m, and q are three positive parameters, and L_i $(i={\rm H,C})$ is the width of the potential field. For the different values of δ, m, and q, two-level quantum engines have different eigenenergies and reversible efficiencies, which are listed in Table 3.[36–41]

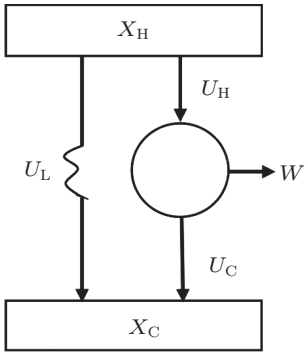


Fig. 1. Schematic diagram of a generalized Carnot cycle with external leakage losses between two reservoirs.

Table 1. Parameters X_i $(i={\rm H,C})$ and $U_{i{\rm r}}$ $(i={\rm H,C})$, and reversible efficiency $\eta_{\rm r,g}$ of generalized Carnot cycles with different potential fields.[41]

Engines	X_i $(i={\rm H,C})$	$\eta_{\rm r,g}$	$U_{i{\rm r}}$ $(i={\rm H,C})$
Carnot heat engine	T_i	$1-T_{\rm C}/T_{\rm H}$	$T_i\Delta S$
Chemical engine	μ_i	$1-\mu_{\rm C}/\mu_{\rm H}$	$\mu_i\Delta N$
Flux flow engine	P_i	$1-P_{\rm C}/P_{\rm H}$	P_iAs
Gravitational engine	H_i	$1-H_{\rm C}/H_{\rm H}$	mgH_i
Quantum heat engine	T_i	$1-T_{\rm C}/T_{\rm H}$	$T_iF(S_1,S_2)$
Non-Carnot engine	T_i	$1-\dfrac{C_{\rm C}(T_2-T_{\rm C})}{C_{\rm H}(T_{\rm H}-T_1)}$	$\pm C_i(T_i-T_j)$
Two-level quantum Carnot engine	E_i	$1-\dfrac{\sigma}{(L_{\rm C}/L_{\rm H})^m}$	$\dfrac{\delta}{L_i^m}[i_2^q-(i_2^q-i_1^q)p_i]\ln\sigma$

Table 2. Expressions of reversible efficiency $\eta_{\rm r,g}$ of several non-Carnot heat engines and the efficiency $\eta_{\rm r,m}$ at the maximum work output.[26,27,40]

$C_{\rm H}/C_{\rm C}$	Cycle modes	$\eta_{\rm r,g}$	$\eta_{\rm r,m}$
1	Brayton (Otto)	$1-\tau T_{\rm H}/T_{\rm l}$	$1-\sqrt{\tau}$
ν	Diesel	$1-\dfrac{\tau[(T_{\rm H}/T_{\rm l})^{\upsilon}-1]}{\upsilon(1-T_{\rm l}/T_{\rm H})}$	$1-\dfrac{\tau^f-\tau}{\nu(1-\tau^f)}$
$1/\nu$	Atkinson	$1-\dfrac{\tau\upsilon[(T_{\rm H}/T_{\rm l})^{1/\upsilon}-1]}{(1-T_{\rm l}/T_{\rm H})}$	$1-\dfrac{\nu(\tau^{1-f}-\tau)}{1-\tau^{1-f}}$
0	Braysson	$1-\dfrac{\tau\ln(T_{\rm H}/T_{\rm l})}{1-T_{\rm l}/T_{\rm H}}$	$1+\dfrac{\tau}{1-\tau}\ln\tau$
∞	unnamed	$1-\dfrac{\tau(T_2/T_{\rm C}-1)}{\ln(T_2/T_{\rm C})}$	$1+\dfrac{1-\tau}{\ln\tau}$

Table 3. Expressions of ε_n, $U_{\rm Hr}$, $U_{\rm Cr}$, and $\eta_{\rm r,g}$ for two-level quantum Carnot engines with different quantum fields.[36–41]

Quantum fields	ε_n $(n=1,2,\ldots)$	$U_{\rm Hr}$	$U_{\rm Cr}$	$\eta_{\rm r,g}$
A single particle trapped in 1D infinite well	$\frac{n^2\pi^2\hbar^2}{2ML^2}$	$\frac{\pi^2\hbar^2(4-3\lvert a_1\rvert^2)}{2ML_{\rm A}^2}\ln\frac{4-3\lvert b_1\rvert^2}{4-3\lvert a_1\rvert^2}$	$-\frac{\pi^2\hbar^2(4-3\lvert b_1\rvert^2)}{2ML_{\rm C}^2}\ln\frac{4-3\lvert b_1\rvert^2}{4-3\lvert a_1\rvert^2}$	$1-\frac{4-3\lvert b_1\rvert^2}{4-3\lvert a_1\rvert^2}\frac{1}{r^2}$, $(r\geq 2)$
A single-mode radiation field in a cavity potential	$\frac{(n-1/2)\hbar s\pi c}{L}$	$\frac{\hbar s\pi c(3-2\lvert a_1\rvert^2)}{2L_{\rm A}}\ln\frac{3-2\lvert b_1\rvert^2}{3-2\lvert a_1\rvert^2}$	$-\frac{\hbar s\pi c(3-2\lvert b_1\rvert^2)}{2L_{\rm C}}\ln\frac{3-2\lvert b_1\rvert^2}{3-2\lvert a_1\rvert^2}$	$1-\frac{3-2\lvert b_1\rvert^2}{3-2\lvert a_1\rvert^2}\frac{1}{r^2}$, $(r\geq 3)$
An extremely relativistic particle in box potential	$\frac{n\pi\hbar c}{L}$	$\frac{\hbar\pi c(2-\lvert a_1\rvert^2)}{L_{\rm A}}\ln\frac{2-\lvert b_1\rvert^2}{2-\lvert a_1\rvert^2}$	$-\frac{\hbar\pi c(2-\lvert b_1\rvert^2)}{L_{\rm C}}\ln\frac{2-\lvert b_1\rvert^2}{2-\lvert a_1\rvert^2}$	$1-\frac{2-\lvert b_1\rvert^2}{2-\lvert a_1\rvert^2}\frac{1}{r^2}$, $(r\geq 2)$

3. Unified cycle model

Under the low-dissipation assumption,[16] for an irreversible generalized Carnot cycle operated between two different potential energy reservoirs, the energies absorbed from the high-potential energy reservoir and released into the low-potential energy reservoir by the working substance per cycle can be expressed respectively as

$$U_{\rm H}=U_{\rm Hr}\left(1-\frac{\sigma_{\rm H}}{t_{\rm H}}\right), \tag{1}$$

$$U_{\rm C}=U_{\rm Cr}\left(1+\frac{\sigma_{\rm C}}{t_{\rm C}}\right), \tag{2}$$

where $U_{\rm Hr}$ and $U_{\rm Cr}$, whose expressions are also listed in Table 1, are the exchange energies between the working substance and the two potential energy reservoirs when the reversible cycle is carried out, $\sigma_{\rm H}$ and $\sigma_{\rm C}$ are two parameters containing the concrete irreversibility, $t_{\rm H}$ and $t_{\rm C}$ are, respectively, the time durations in which the working substance contacts with the high- and low-potential energy reservoirs. This assumption means that compared with energy transfer times $t_{\rm H}$ and $t_{\rm C}$, the relaxation time of the working substance in the cycle is very fast, and that, by ignoring complicated time-dependent terms due to the non-equilibrium between the reservoirs and the working substance, energy dissipations are expected to behave as $\sigma_{\rm H}/t_{\rm H}$ and $\sigma_{\rm C}/t_{\rm C}$ along high- and low-potential energy segments of the cycle. It is seen from Eqs. (1) and (2) that the cycle will return to reversibility when $t_{\rm H}\to\infty$ and $t_{\rm C}\to\infty$. Compared with $t_{\rm H}$ and $t_{\rm C}$, the times spent in two processes without energy exchange are further assumed to be negligible. Thus, the time spent in finishing one cycle may be approximately expressed as $t=t_{\rm H}+t_{\rm C}$.

Usually, the external leakage losses inevitably occur between two potential energy reservoirs and will affect the performance of the cycle. The external leakage losses per cycle $U_{\rm L}$ shown in Fig. 1 may be simply described by

$$U_{\rm L}=u_{\rm L}t=u_{\rm L}(t_{\rm H}+t_{\rm C}), \tag{3}$$

where $u_{\rm L}$ is the rate of the external leakage losses from the high-potential energy reservoir to the low-potential energy reservoir. In general, $u_{\rm L}$ is dependent on the energy reservoir and will have different values for different energy reservoirs. However, $u_{\rm L}$ can be regarded as a constant for given energy reservoirs. Using Eqs. (1)–(3), we can derive the power output P and the efficiency η of the generalized Carnot cycle with the external leakage losses as

$$\begin{aligned} P &= \frac{U_{\rm H}+U_{\rm L}-(U_{\rm C}+U_{\rm L})}{t_{\rm H}+t_{\rm C}} \\ &= \frac{U_{\rm Hr}-U_{\rm Cr}-U_{\rm Hr}\sigma_{\rm H}/t_{\rm H}-U_{\rm Cr}\sigma_{\rm C}/t_{\rm C}}{t_{\rm H}+t_{\rm C}}, \end{aligned} \tag{4}$$

$$\begin{aligned} \eta &= \frac{U_{\rm H}+U_{\rm L}-(U_{\rm C}+U_{\rm L})}{U_{\rm H}+U_{\rm L}} \\ &= \frac{U_{\rm Hr}-U_{\rm Cr}-U_{\rm Hr}\sigma_{\rm H}/t_{\rm H}-U_{\rm Cr}\sigma_{\rm C}/t_{\rm C}}{U_{\rm Hr}(1-\sigma_{\rm H}/t_{\rm H})+u_{\rm L}(t_{\rm H}+t_{\rm C})}. \end{aligned} \tag{5}$$

Using Eqs. (4) and (5), one can discuss the performance characteristics of low-dissipative generalized Carnot cycles with external leakage losses between the two reservoirs.

4. Optimal relations between power output and efficiency

In order to obtain the optimal relations between the power output and the efficiency of low-dissipative generalized Carnot cycles with external leakage losses, we introduce the Lagrangian function

$$\begin{aligned} L &= P+\lambda\left(\eta-\frac{U_{\rm H}-U_{\rm C}}{U_{\rm H}+U_{\rm L}}\right) \\ &= \frac{U_{\rm Hr}-U_{\rm Cr}-\dfrac{U_{\rm Hr}\sigma_{\rm H}}{t_{\rm H}}-\dfrac{U_{\rm Cr}\sigma_{\rm C}}{t_{\rm C}}}{t_{\rm H}+t_{\rm C}} \\ &\quad +\lambda\left[\eta-\frac{U_{\rm Hr}-U_{\rm Cr}-\dfrac{U_{\rm Hr}\sigma_{\rm H}}{t_{\rm H}}-\dfrac{U_{\rm Cr}\sigma_{\rm C}}{t_{\rm C}}}{U_{\rm Hr}(1-\sigma_{\rm H}/t_{\rm H})+q_{\rm L}(t_{\rm H}+t_{\rm C})}\right], \end{aligned} \tag{6}$$

where λ is the Lagrangian multiplier. By using Eq. (6) and the Euler–Lagrange equations $\partial L/\partial t_{\rm H}=0$ and $\partial L/\partial t_{\rm C}=0$, an important relation

$$\sigma_{\rm H}t_{\rm C}^2-\sigma_{\rm C}t_{\rm H}^2+2(t_{\rm H}+t_{\rm C})\sigma_{\rm H}\sigma_{\rm C}=0 \tag{7}$$

is obtained. Equation (7) can be solved as

$$\begin{cases} t_{\rm C}=\sigma_{\rm C}(c-1), & (\sigma_{\rm H}\neq 0), \\ t_{\rm H}=\sigma_{\rm H}(c'-1), & (\sigma_{\rm C}\neq 0), \end{cases} \tag{8}$$

where $c=\sqrt{1-2x/\alpha+x^2/\alpha}$, $c'=\sqrt{1+2\alpha X+\alpha X^2}$, $\alpha=\sigma_C/\sigma_H$, $x=t_H/\sigma_H$, and $X=t_C/\sigma_C$. By substituting Eq. (8) into Eqs. (4) and (5), both the power output and the efficiency can be expressed as functions of x or X, namely,

$$P=\begin{cases}\dfrac{U_{Hr}}{\sigma_H}\dfrac{\eta_{r,g}-1/x-(1-\eta_{r,g})/(c-1)}{x+\alpha(c-1)}, & (\sigma_H\neq 0),\\ \dfrac{U_{Hr}}{\sigma_C}\dfrac{\eta_{r,g}-1/(c'-1)-(1-\eta_{r,g})/X}{X+(c'-1)/\alpha}, & (\sigma_C\neq 0),\end{cases} \tag{9}$$

$$\eta=\begin{cases}\dfrac{\eta_{r,g}-1/x-(1-\eta_{r,g})/(c-1)}{1-1/x+k[x+\alpha(c-1)]}, & (\sigma_H\neq 0),\\ \dfrac{\eta_{r,g}-1/(c'-1)-(1-\eta_{r,g})/X}{1-1/(c'-1)+K[(c'-1)/\alpha+X]}, & (\sigma_C\neq 0),\end{cases} \tag{10}$$

where $\eta_{r,g}=1-U_{Cr}/U_{Hr}$, $k=u_L\sigma_H/U_{Hr}$, and $K=u_L\sigma_C/U_{Hr}$. By using Eqs. (9) and (10), the general characteristic curves of the power output varying with the efficiency can be generated with the help of a numerical calculation, as shown in Fig. 2, where the controlling parameter is x or X, $P^*=P/P_{max}$ is the normalized power output, and the parabolic-shaped and loop-shaped curves correspond to the cases of $k=0$ or $K=0$, and $k\neq 0$ or $K\neq 0$, respectively. When $0<\alpha<\infty$, $K=\alpha k$, and consequently, the first and second equations in Eq. (9) or (10) are equivalent to each other. When $\alpha=0$ or $\alpha\to\infty$, both k and K may have the same values because they correspond to different curves, respectively.

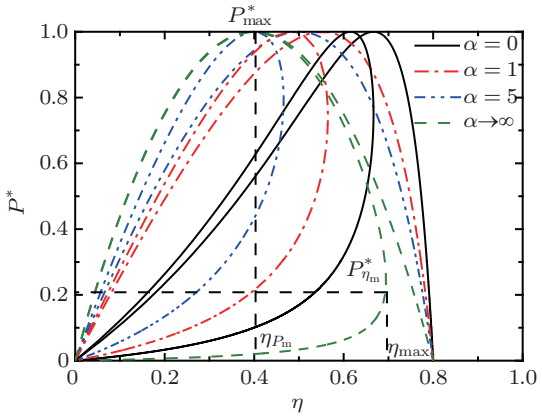


Fig. 2. (color online) Curves of the dimensionless power output P^* versus η for different values of α, where $\eta_{r,g}=0.8$, and $k=0$ and 0.02. When $\alpha\to\infty$, the value of K is chosen to be equal to that of k, respectively.

It can be clearly seen from Fig. 2 that when the external leakage losses between two reservoirs are negligible, the η–P^* characteristic curves are parabolic. The power output is equal to zero when the efficiency reaches the reversible efficiency $\eta_{r,g}$. When the influence of external leakage losses between two reservoirs is considered, the η–P^* characteristic curves become looped shapes. The maximum efficiency η_{max} is smaller than $\eta_{r,g}$, and the power output at the maximum efficiency is larger than zero. For a given value of k or K, the efficiency at the maximum power output increases with the decrease of α, and for a given value of α, the efficiency at the maximum power output with external leakage losses between two reservoirs is always smaller than that without external leakage losses. Figure 2 also shows that when the efficiency is smaller than η_{P_m}, the power output of generalized Carnot cycles decreases with the decrease of the efficiency, and when the power output is smaller than $P^*_{\eta_m}$, the efficiency of the generalized Carnot cycle also decreases with the decrease of power output. Obviously, the regions of $P^*<P^*_{\eta_m}$ and $\eta<\eta_{P_m}$ are not optimal for the generalized Carnot cycle. Thus, the optimal regions of generalized Carnot cycles should be $P^*_{max}\geq P^*\geq P^*_{\eta_m}$ and $\eta_{max}\geq\eta\geq\eta_{P_m}$. According to the two criteria given above, we can further determine the optimal regions of x and X as $x_{\eta_m}\geq x\geq x_{P_m}$ and $X_{\eta_m}\geq X\geq X_{P_m}$, from which we can directly give the optimal criteria of t_H and t_C as $x_{\eta_m}\sigma_H\geq t_H\geq x_{P_m}\sigma_H$ and $X_{\eta_m}\sigma_C\geq t_C\geq X_{P_m}\sigma_C$, where x_{P_m} and X_{P_m} are the values of x and X at the maximum power output and x_{η_m} and X_{η_m} are the values of x and X at the maximum efficiency, respectively, x_{P_m}, X_{P_m}, x_{η_m}, and X_{η_m} will be given by some equations of Sections 5 and 6.

It is significant to note that for some special values of α, some simple expressions of the power output and efficiency may be directly derived from Eqs. (9) and (10). For instance, when $\alpha\to 0$ and σ_H is finite, the power output and the efficiency can be expressed as

$$\begin{cases}P_0=\dfrac{U_{Hr}}{\sigma_H}\dfrac{\eta_{r,g}-1/x}{x},\\ \eta_0=\dfrac{\eta_{r,g}-1/x}{1-1/x+kx}.\end{cases} \tag{11}$$

When $\alpha=1$, i.e., σ_H=σ_C, the power output and the efficiency are given by

$$\begin{cases}P_1=\dfrac{U_{Hr}}{\sigma_H}\dfrac{\eta_{r,g}-2/x}{2(x-2)},\\ \eta_1=\dfrac{\eta_{r,g}-2/x}{(x-2)(1/x+2k)},\end{cases} \tag{12}$$

which correspond to the so-called symmetric dissipation.[16] When $\alpha\to\infty$ and σ_C is finite, the power output and the efficiency can be obtained as

$$\begin{cases}P_\infty=\dfrac{U_{Hr}}{\sigma_C}\dfrac{\eta_{r,g}-(1-\eta_{r,g})/X}{X},\\ \eta_\infty=\dfrac{\eta_{r,g}-(1-\eta_{r,g})/X}{1+KX}.\end{cases} \tag{13}$$

5. Efficiency at the maximum power output

From Eq. (9) and $dP/d\eta=0$, it can be proved that when

$$\begin{cases}x=\dfrac{2}{\eta_{r,g}}[1+\sqrt{\alpha(1-\eta_{r,g})}]\equiv x_{P_m}, & \alpha \text{ is finite},\\ X=\dfrac{2(1-\eta_{r,g})}{\eta_{r,g}}\equiv X_{P_m}, & \alpha\to\infty,\end{cases} \tag{14}$$

the power output attains its maximum, i.e.,

$$P_{\max}=\begin{cases}\dfrac{U_{\rm Hr}}{\sigma_{\rm H}}\dfrac{\eta_{\rm r,g}-\eta_{\rm r,g}/2[1+\sqrt{\alpha(1-\eta_{\rm r,g})}]-(1-\eta_{\rm r,g})/(C-1)}{2[1+\sqrt{\alpha(1-\eta_{\rm r,g})}]/\eta_{\rm r,g}+\alpha(C-1)}, & \alpha \text{ is finite},\\ \dfrac{U_{\rm Hr}}{\sigma_{\rm C}}\left(\dfrac{\eta_{\rm r,g}}{2\sqrt{1-\eta_{\rm r,g}}}\right)^2, & \alpha\to\infty,\end{cases} \tag{15}$$

and the corresponding efficiency is given by

$$\eta_{p_{\rm m}}=\begin{cases}\dfrac{\eta_{\rm r,g}-\eta_{\rm r,g}/2[1+\sqrt{\alpha(1-\eta_{\rm r,g})}]-(1-\eta_{\rm r,g})/(C-1)}{1-\eta_{\rm r,g}/2[1+\sqrt{\alpha(1-\eta_{\rm r,g})}]+k\{2[1+\sqrt{\alpha(1-\eta_{\rm r,g})}]/\eta_{\rm r,g}+\alpha(C-1)\}}, & \alpha \text{ is finite},\\ \dfrac{\eta_{\rm r,g}}{2+4K(1-\eta_{\rm r,g})/\eta_{\rm r,g}}, & \alpha\to\infty,\end{cases} \tag{16}$$

where

$$C=\{4[1+\sqrt{\alpha(1-\eta_{\rm r,g})}]^2/\alpha\eta_{\rm r,g}^2 -4[1+\sqrt{\alpha(1-\eta_{\rm r,g})}]/\alpha\eta_{\rm r,g}+1\}^{1/2}.$$

By using Eqs. (15) and (16), the $\eta_{\rm r,g}$–$P^*_{\max}$ and $\eta_{\rm r,g}$–$\eta_{P_{\rm m}}$ curves for different values of k or K can be plotted as shown in Figs. 3 and 4, respectively.

Figure 3 shows that $P^*_{\max}$ decreases with the increased value of α in the same value of $\eta_{\rm r,g}$, namely, $P^*_{m,0}>P^*_{m,1}>P^*_{m,\infty}$, which means that $P^*_{m,0}$ can be regard as the limit of the maximum power output. From Fig. 4(a), it can be identified that $\eta_{p_{\rm m},0}$ and $\eta_{p_{\rm m},\infty}$ are the upper and lower bound of the efficiency at the maximum power output without external leakage losses between the two reservoirs. In this condition, for any other specific value of α, $\eta_{p_{\rm m},\rm others}$ is restricted between $\eta_{p_{\rm m},0}$ and $\eta_{p_{\rm m},\infty}$. It is seen from Figs. 4(b)–4(d) that the curves with $k\neq 0$ or $K\neq 0$ decline with the increase of external leakage losses, but the decreasing rate of the curve of $\eta_{p_{\rm m},\infty}$ is smaller than that of the others, which leads to $\eta_{p_{\rm m},\infty}>\eta_{p_{\rm m},0}$ as shown in Fig. 4(d). In other words, $\eta_{p_{\rm m},0}$ may be regarded as the upper bound of the efficiency at the maximum power output when external leakage losses are not obvious. When external leakage losses increase, the efficiency at the maximum power output will decrease and $\eta_{p_{\rm m},\infty}$ will replace $\eta_{p_{\rm m},0}$ as the upper bound of the efficiency at the maximum power output. Figure 4 also shows that $\eta_{p_{\rm m},0}$ with $k=0$ is always larger than any other efficiency at the maximum power output and is the upper bound of the efficiency at the maximum power output for the low-dissipative generalized Carnot cycle with external leakage losses.

Besides, for some special values of α, the expressions of the maximum power output and the corresponding efficiency can be obtained by using Eqs. (15) and (16). For example, when $\alpha\to 0$, the maximum power output and the corresponding efficiency can be simplified into

$$P_{\rm m,0}=\frac{U_{\rm Hr}}{\sigma_{\rm H}}\left(\frac{\eta_{\rm r,g}}{2}\right)^2, \tag{17}$$

$$\eta_{p_{\rm m},0}=\frac{\eta_{\rm r,g}}{2-\eta_{\rm r,g}+4k/\eta_{\rm r,g}}. \tag{18}$$

When $\alpha=1$, the maximum power output and the corresponding efficiency are derived as

$$P_{\rm m,1}=\frac{U_{\rm Hr}}{\sigma_{\rm H}}\left[\frac{\eta_{\rm r,g}}{2(1+\sqrt{1-\eta_{\rm r,g}})}\right]^2, \tag{19}$$

$$\eta_{p_{\rm m},1}=\frac{1-\sqrt{1-\eta_{\rm r,g}}}{1+4k(1+\sqrt{1-\eta_{\rm r,g}})/\eta_{\rm r,g}}. \tag{20}$$

When $\alpha\to\infty$, the maximum power output and the corresponding efficiency are given by

$$P_{\rm m,\infty}=\frac{U_{\rm Hr}}{\sigma_{\rm C}}\left(\frac{\eta_{\rm r,g}}{2\sqrt{1-\eta_{\rm r,g}}}\right)^2, \tag{21}$$

$$\eta_{p_{\rm m},\infty}=\frac{\eta_{\rm r,g}}{2+4K(1-\eta_{\rm r,g})/\eta_{\rm r,g}}. \tag{22}$$

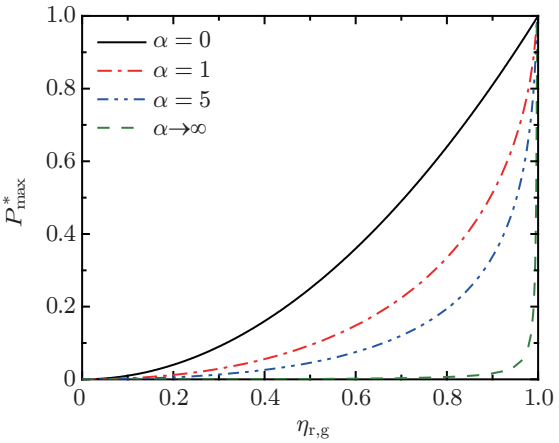


Fig. 3. (color online) Curves of the maximum power output $P^*_{\max}$ versus reversible efficiency $\eta_{\rm r,g}$ for different values of α.

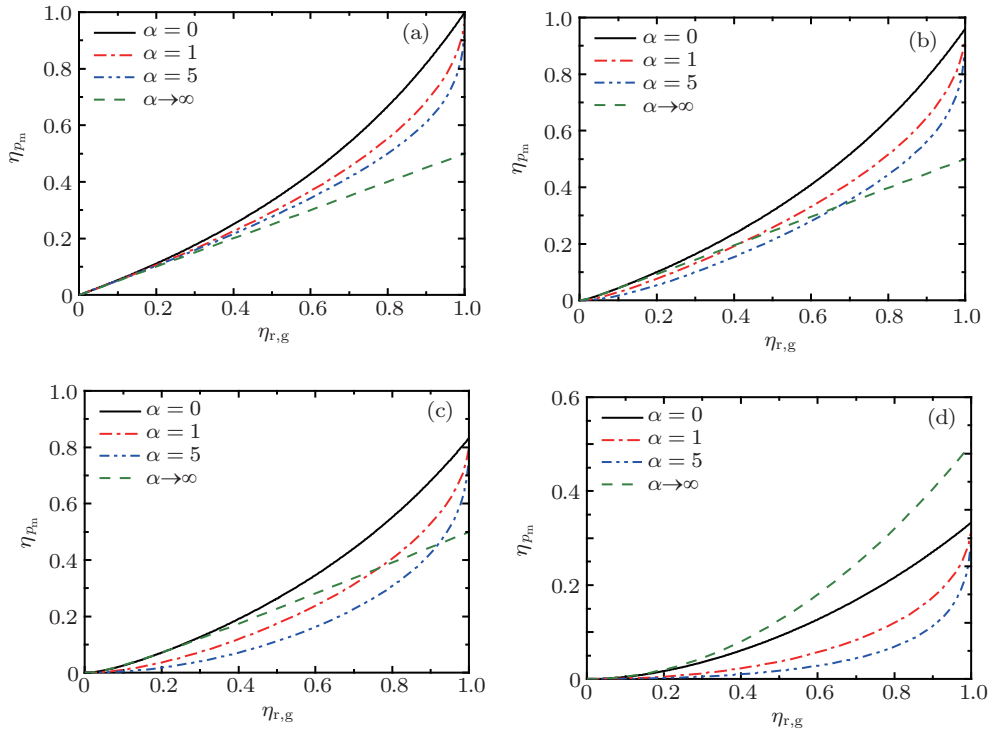


Fig. 4. (color online) Variations of the efficiency at the maximum power output with reversible efficiency $\eta_{r,g}$ for different values of α and k, where (a) $k = 0$, (b) $k = 0.01$, (c) $k = 0.05$, and (d) $k = 0.5$. In panels (a)–(d), when $\alpha \to \infty$, the value of K is chosen to be equal to that of k, respectively.

6. Power output at maximum efficiency

It can be found from Fig. 2 that there exists not only a maximum power output but also a maximum efficiency for the generalized Carnot cycles with external leakage losses. According to Eq. (10) and $\mathrm{d}\eta/\mathrm{d}P = 0$, one can derive a relation as

$$\begin{cases} \left[\dfrac{1}{x^2} + \dfrac{(x-1)(1-\eta_{r,g})}{\alpha c(c-1)}\right]\left\{1 - \dfrac{1}{x} + k[x + \alpha(c-1)]\right\} \\ -\left[\dfrac{1}{x^2} + k\left(\dfrac{x-1}{c} + 1\right)\right]\left(\eta_{r,g} - \dfrac{1}{x} - \dfrac{1-\eta_{r,g}}{c-1}\right) = 0, \\ \alpha \text{ is finite}, \\ \dfrac{(1-\eta_{r,g})(1+KX)}{X^2} - K\left[\eta_{r,g} - \dfrac{1-\eta_{r,g}}{X}\right] = 0, \\ \alpha \to \infty. \end{cases} \tag{23}$$

For general cases, we can obtain the values x_{η_m} and X_{η_m} of x and X at the maximum efficiency by using Eq. (23) and the numerical calculation. For some special values of α, equation (23) is solvable. For example, when $\alpha = 0$, we obtain

$$x_0 = \frac{c_0 + 1}{\eta_{r,g}} \equiv x_{\eta_m,0}, \tag{24}$$

where $c_0 = \sqrt{1 - \eta_{r,g}^2/k + \eta_{r,g}/k}$. The maximum efficiency and the corresponding power output can be expressed as

$$\eta_{m,0} = \frac{\eta_{r,g} - \eta_{r,g}/(c_0+1)}{1 - \eta_{r,g}/(c_0+1) + k(c_0+1)/\eta_{r,g}}, \tag{25}$$

$$P_{\eta_m,0} = \frac{U_{Hr}}{\sigma_H}\frac{c_0\eta_{r,g}^2}{(c_0+1)^2}. \tag{26}$$

When $\alpha = 1$, the solution is given by

$$x_1 = \frac{c_1 + 2}{\eta_{r,g}} \equiv x_{\eta_m,1}, \tag{27}$$

where $c_1 = \sqrt{(1-\eta_{r,g})(4 + \eta_{r,g}/k)}$. The maximum efficiency and the corresponding power output can be expressed as

$$\eta_{m,1} = \frac{c_1\eta_{r,g}^2}{[c_1 + 2(1-\eta_{r,g})][\eta_{r,g} + 2k(c_1+2)]}, \tag{28}$$

$$P_{\eta_m,1} = \frac{U_{Hr}}{\sigma_H}\frac{\eta_{r,g}^2[1 - 2/(c_1+2)]}{2[c_1 + 2(1-\eta_{r,g})]}. \tag{29}$$

For $\alpha \to \infty$, from the second equation of Eq. (23), we derive

$$X = \frac{c_\infty + (1-\eta_{r,g})}{\eta_{r,g}} \equiv X_{\eta_m,\infty}, \tag{30}$$

where $c_\infty = \sqrt{(1-\eta_{r,g})(1 - \eta_{r,g} + \eta_{r,g}/K)}$. The maximum efficiency and the corresponding power output can be expressed as

$$\eta_{m,\infty} = \frac{c_\infty\eta_{r,g}^2}{(c_\infty + 1 - \eta_{r,g})[\eta_{r,g} + K(c_\infty + 1 - \eta_{r,g})]}, \tag{31}$$

$$P_{\eta_m,\infty} = \frac{U_{Hr}}{\sigma_C}\frac{c_\infty\eta_{r,g}^2}{(c_\infty + 1 - \eta_{r,g})^2}. \tag{32}$$

By using the above equations, the $\eta_{r,g}$–$P^*_{\eta_m}$ and $\eta_{r,g}$–η_{max} curves can be generated as shown in Fig. 5. The positions of these curves depend on not only the value of α but also the value of k or K.

Figures 5(a) and 5(c) show that when $k = K = 0.01$ and $k = K = 0.1$, $P^*_{\eta_{m,0}}$ is larger than $P^*_{\eta_{m,1}}$ and $P^*_{\eta_{m,\infty}}$. It can be proved from Eqs. (26) and (32) that $P^*_{\eta_{m,0}}$ is larger than $P^*_{\eta_{m,\infty}}$ for any finite value of $k = K$. Thus, we can take $P^*_{\eta_{m,0}}$ as the upper bound of the power output at the maximum efficiency. It is found from Fig. 5(b) that when the external leakage losses are not obvious, i.e. the value of k or K is very small, the efficiencies of generalized Carnot cycles satisfy $\eta_{r,g} \approx \eta_{m,\infty} \approx \eta_{m,0}$. Comparing Fig. 5(b) with Fig. 5(d), it is noted that the curves of η_{max} decline with the increase of external leakage losses for a given value of α, and the decreasing rate of the curve of $\alpha \to \infty$ is smaller than those of other curves, which leads to $\eta_{m,\infty} > \eta_{m,0}$ when external leakage losses are large enough.

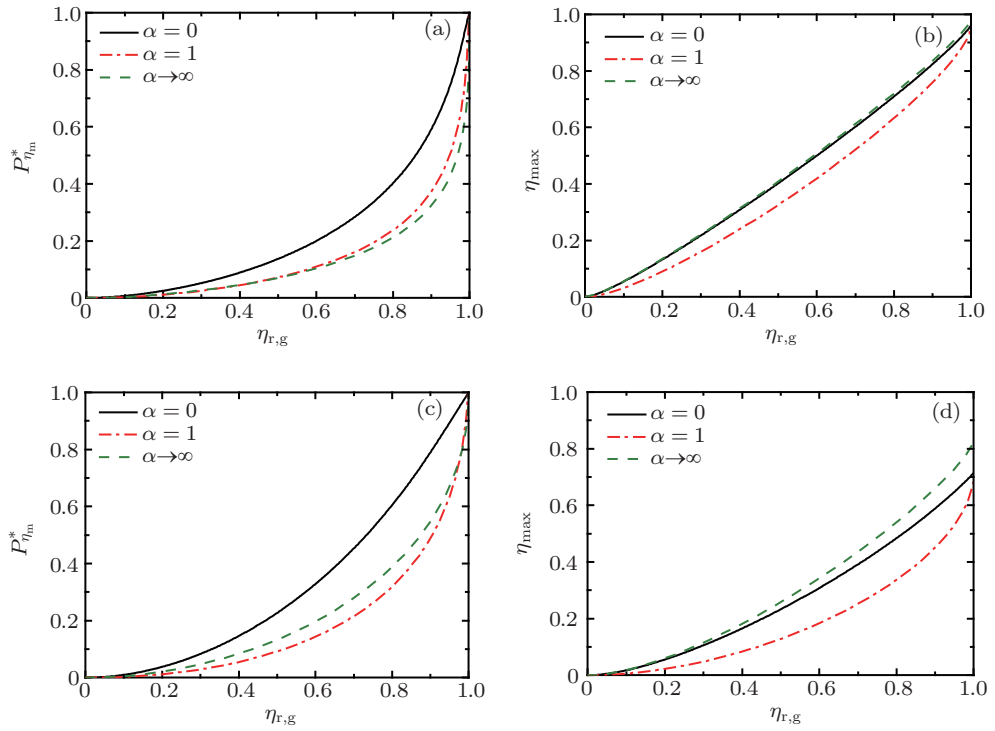


Fig. 5. (color online) Variations of the maximum efficiency and the corresponding power output with reversible efficiency $\eta_{r,g}$ for different values of α and k: $k = 0.01$ ((a) and (b)) and $k = 0.1$ ((c) and (d)). In panels (a)–(d), when $\alpha \to \infty$, the value of K is chosen to be equal to that of k, respectively.

7. Discussion

By using the results obtained above and Tables 1–3, we can directly discuss the performance characteristics of various generalized Carnot cycles. For example, for a low-dissipative Carnot heat engine with heat leakage losses between the two heat reservoirs, we can obtain the performance characteristics of the heat engine as long as one chooses $U_H = Q_H$, $U_C = Q_C$, $U_L = Q_L$, $U_{Hr} = Q_{Hr} = T_H\Delta S$, $U_{Cr} = Q_{Cr} = T_C\Delta S$, and $u_L = q_L$, where ΔS is the entropy change of the working substance in the isothermal heat exchange process and q_L is the rate of the heat leakage losses between two heat reservoirs. For some special values of α, we easily obtain the analytical expressions of the maximum power output P_{max} and the corresponding efficiency η_{P_m}, and the maximum efficiency η_{max} and the corresponding power output P_{η_m} of the low-dissipative Carnot heat engine with heat leakage losses, which are listed in Table 4, where $k_c = q_L\sigma_H/Q_{Hr}$, $K_c = q_L\sigma_C/Q_{Hr}$, and $\eta_{r,g} = 1 - T_C/T_H \equiv \eta_r$. If the heat leakage losses between two heat reservoirs are negligible, the optimal relations between the power output and the efficiency can be further simplified into

$$P_{c,0} = \frac{T_H\Delta S}{\sigma_H}\frac{\eta(\eta_r - \eta)(1-\eta_r)}{(1-\eta)^2}, \tag{33}$$

$$P_{c,1} = \frac{T_H\Delta S}{\sigma_H}\frac{\eta(\eta_r - \eta)}{4(1-\eta)}, \tag{34}$$

$$P_{c,\infty} = \frac{T_H\Delta S}{\sigma_C}\frac{\eta(\eta_r - \eta)}{(1-\eta_r)}, \tag{35}$$

which are exactly the results obtained in Refs. [21] and [41]. The efficiency at the maximum power output is given by

$$\eta_{c,0} = \frac{\eta_r}{2}, \tag{36}$$

$$\eta_{c,1} = 1 - \sqrt{1-\eta_r} \equiv \eta_{CA}, \tag{37}$$

$$\eta_{c,\infty} = \frac{\eta_r}{2-\eta_r}, \tag{38}$$

respectively, which are the results obtained in Ref. [16]. For other kinds of low-dissipative generalized Carnot cycles with external leakage losses, similar discussion may be carried out by using the above universal results and Tables 1–3.

Table 4. Expressions of some parameters of the low-dissipative Carnot heat engine with heat leakage losses for different values of α.

α	$P_{\max}$	$\eta_{P_{\max}}$	$\eta_{\max}$	$P_{\eta_{\max}}$
$\alpha \to 0$	$\frac{Q_{\rm Hr}}{\sigma_{\rm H}}\left(\frac{\eta_{\rm r}}{2}\right)^2$	$\frac{\eta_{\rm r}}{2-\eta_{\rm r}+4k_{\rm c}/\eta_{\rm r}}$	$\frac{\eta_{\rm r}-\eta_{\rm r}/(c_{\rm c,0}+1)}{1-\eta_{\rm r}/(c_{\rm c,0}+1)+k_{\rm c}(c_{\rm c,0}+1)/\eta_{\rm r}}$	$\frac{Q_{\rm Hr}}{\sigma_{\rm H}}\frac{c_{\rm c,0}\eta_{\rm r}^2}{(c_{\rm c,0}+1)^2}$
$\alpha = 1$	$\frac{Q_{\rm Hr}}{\sigma_{\rm H}}\left[\frac{\eta_{\rm r}}{2(1+\sqrt{1-\eta_{\rm r}})}\right]^2$	$\frac{1-\sqrt{1-\eta_{\rm r}}}{1+4k_{\rm c}(1+\sqrt{1-\eta_{\rm r}})/\eta_{\rm r}}$	$\frac{c_{\rm c,1}\eta_{\rm r}^2}{[c_{\rm c,1}+2(1-\eta_{\rm r})][\eta_{\rm r}+2k_{\rm c}(c_{\rm c,1}+2)]}$	$\frac{Q_{\rm Hr}}{\sigma_{\rm H}}\frac{\eta_{\rm r}^2[1-2/(c_{\rm c,1}+2)]}{2[c_{\rm c,1}+2(1-\eta_{\rm r})]}$
$\alpha \to \infty$	$\frac{Q_{\rm Hr}}{\sigma_{\rm C}}\left(\frac{\eta_{\rm r}}{2\sqrt{1-\eta_{\rm r}}}\right)^2$	$\frac{\eta_{\rm r}}{2+4K_{\rm c}(1-\eta_{\rm r})/\eta_{\rm r}}$	$\frac{c_{\rm c,\infty}\eta_{\rm r}^2}{(c_{\rm c,\infty}+1-\eta_{\rm r})[\eta_{\rm r}+K_{\rm c}(c_{\rm c,\infty}+1-\eta_{\rm r})]}$	$\frac{Q_{\rm Hr}}{\sigma_{\rm C}}\frac{c_{\rm c,\infty}\eta_{\rm r}^2}{(c_{\rm c,\infty}+1-\eta_{\rm r})^2}$

Entropy production is often taken as an objective function in thermodynamic cycle optimizations.[54–56] According to the above analyses, one can derive the entropy production per cycle for a low-dissipative Carnot heat engine as

$$\sigma = (Q_{\rm H}+Q_{\rm L})(\eta_{\rm r}-\eta)/T_{\rm C}. \tag{39}$$

It is seen from Eq. (39) that when $\eta = \eta_{\rm r}$, then $\sigma = 0$. This means that if the maximum efficiency of a system can attain the Carnot efficiency, the state of the minimum entropy production corresponds to that of the maximum efficiency. If the maximum efficiency of a system is smaller than the Carnot efficiency, the minimum entropy production depends on both η and $(Q_{\rm H}+Q_{\rm L})$, and consequently, the state of the minimum entropy production is different from that of the maximum efficiency. Using Eq. (39), one can further obtain the relation between the entropy production rate and the power output as

$$\dot{\sigma} = P(\eta_{\rm r}/\eta - 1)/T_{\rm C}. \tag{40}$$

It is seen from Eq. (40) that the entropy production rate depends on both the efficiency and the power output. Thus, the state of the minimum entropy production rate is, in general, different from that of the maximum power output.

8. Conclusions

We have established the model of low-dissipative generalized Carnot cycles with external leakage losses, which may include several classes of typical engines, such as Carnot heat engines, Carnot-like engines, Carnot chemical engines, two-level quantum Carnot engines, etc. The expressions of the power output and efficiency are derived, and the optimal relations between them are discussed. The optimal operating regions are determined. The performance characteristics at the maximum power output and efficiency are analyzed. It is also expounded that like the efficiency and power output, the entropy production may be taken as an objective function of a thermodynamic system. There exist some certain relations between the entropy production and the efficiency and between the entropy production rate and the power output, but for general cases, the state of the minimum entropy production is different from that of the maximum efficiency and the state of the minimum entropy production rate is different from that of the maximum power output. The results obtained are universal, from which not only some important conclusions in the literature may be derived but also some novel results can be obtained.

References

[1] Linke H, Humphrey T E, Löfgren A, Sushkov A O, Newbury R, Taylor R P and Omling P 1999 *Science* **286** 2314
[2] Blickle V and Bechinger C 2012 *Nat. Phys.* **8** 143
[3] Fialko O and Hallwood D W 2012 *Phys. Rev. Lett.* **108** 085303
[4] He J, Li Cong and Zhang Y 2013 *Chin. Phys. Lett.* **30** 100501
[5] Zhang Y and He J 2013 *Chin. Phys. Lett.* **30** 010501
[6] Xiao Y, He J and Cheng H 2014 *Acta Phys. Sin.* **63** 200501 (in Chinese)
[7] Li J, Chen L, Ge Y and Sun F 2013 *Acta Phys. Sin.* **62** 130501 (in Chinese)
[8] Liu N, Luo X and Zhang M 2014 *Chin. Phys. B* **23** 080502
[9] Cheng X T and Liang X G 2015 *Chin. Phys. B* **24** 060510
[10] van den Broeck C 2005 *Phys. Rev. Lett.* **95** 190602
[11] Esposito M, Lindenberg K and van den Broeck C 2009 *Phys. Rev. Lett.* **102** 130602
[12] Esposito M, Lindenberg K and van den Broeck C 2009 *Europhys. Lett.* **85** 60010
[13] Izumida Y and Okuda K 2012 *Europhys. Lett.* **97** 10004
[14] Izumida Y and Ito N 2013 *Eur. Phys. J. B* **86** 431
[15] Tu Z C 2012 *Chin. Phys. B* **21** 020513
[16] Esposito M, Kawai R, Lindenberg K and van den Broeck C 2010 *Phys. Rev. Lett.* **105** 150603
[17] Sheng S and Tu Z C 2013 *J. Phys. A: Math. Theor.* **46** 402001
[18] Curzon F L and Ahlborn B 1975 *Am. J. Phys.* **43** 22
[19] de Tomás C, Hernández A C and Roco J M M 2012 *Phys. Rev. E* **85** 010104
[20] Wang Y, Li M, Tu Z C, Hernández A C and Roco J M M 2012 *Phys. Rev. E* **86** 011127
[21] Guo J, Wang Y and Chen J 2012 *J. Appl. Phys.* **112** 103504
[22] Guo J, Wang J, Wang Y and Chen J 2013 *J. Appl. Phys.* **113** 143510
[23] Gordon J M 1991 *Am. J. Phys.* **59** 551
[24] Izumida Y, Okuda K, Hernández A C and Roco J M M 2013 *Europhys. Lett.* **101** 10005
[25] Chen J 1994 *J. Phys. D: Appl. Phys.* **27** 1144
[26] Leff H S 1987 *Am. J. Phys.* **55** 602
[27] Landsberg P T and Leff H S 1989 *J. Phys. A: Math. Gen.* **22** 4019
[28] Zhang Y, Lin B and Chen J 2005 *J. Appl. Phys.* **97** 084905
[29] Bejan A 1996 *Int. J. Heat Mass Transfer* **39** 1175
[30] Chen L, Bi Y and Wu C 1999 *J. Phys. D: Appl. Phys.* **32** 1346
[31] Hu W and Chen J 2006 *J. Phys. D: Appl. Phys.* **39** 993
[32] De Vos A 1991 *J. Phys. Chem.* **95** 4534
[33] Gordon J M and Orlov V N 1993 *J. Appl. Phys.* **74** 5303
[34] Lin G, Chen J and Brück E 2004 *Appl. Energ.* **78** 123
[35] Xia S, Chen L and Sun F 2009 *J. Appl. Phys.* **105** 124905
[36] Bender C M, Brody D C and Meister B K 2000 *J. Phys. A: Math. Gen.* **33** 4427

[37] Abe S 2011 *Phys. Rev. E* **83** 041117
[38] Abe S and Okuyama S 2011 *Phys. Rev. E* **83** 021121
[39] Abe S and Okuyama S 2012 *Phys. Rev. E* **85** 011104
[40] Wang J and He J 2012 *J. Appl. Phys.* **111** 043505
[41] Guo J, Wang J, Wang Y and Chen J 2013 *Phys. Rev. E* **87** 012133
[42] Ge Y, Chen L and Sun F 2008 *Appl. Energy* **85** 618
[43] Chen L, Zheng T, Sun F and Wu C 2003 *Int. J. Ambient Energy* **24** 195
[44] Zhang Y, Ou C, Lin B and Chen J 2005 *J. Energy Res. Technol.* **128** 216
[45] Zhou Y, Tyagi S K, Wu C and Chen J 2005 *Int. J. Ambient Energy* **26** 37
[46] Wu C and Kiang R L 1990 *Int. J. Ambient Energy* **11** 129
[47] Chen L, Lin J, Luo J, Sun F and Wu C 2002 *Int. J. Energy Res.* **26** 965
[48] Zhao Y, Lin B, Zhang Y and Chen J 2006 *Energy Convers. Manage.* **47** 3383
[49] Zhao Y and Chen J 2006 *Appl. Energy* **83** 789
[50] Ge Y, Chen L, Sun F and Wu C 2007 *J. Energy Inst.* **80** 52
[51] Geva E and Kosloff R 1992 *J. Chem. Phys.* **97** 4398
[52] Geva E and Kosloff R 1992 *J. Chem. Phys.* **96** 3054
[53] Wu F, Chen L, Wu S, Sun F and Wu C 2006 *J. Chem. Phys.* **124** 214702
[54] Cheng X and Liang X 2013 *Chin. Phys. B* **22** 010508
[55] Zhou B, Cheng X and Liang X 2013 *Chin. Phys. B* **22** 084401
[56] Wang W, Cheng X and Liang X 2013 *Chin. Phys. B* **22** 110506